

Long-lived radionuclides in ferromanganese crusts

Dominik Koll^{1,2,3,*}, Sebastian Fichter¹, Johannes Lachner¹, Georg Rugel¹, and Anton Wallner^{1,2,3}

¹Accelerator Mass Spectrometry and Isotope Research, Helmholtz-Zentrum Dresden-Rossendorf, 01328 Dresden, Germany.

²Department of Nuclear Physics and Accelerator Applications, The Australian National University, 2600 Canberra, Australia.

³Institute of Nuclear and Particle Physics, TUD Dresden University of Technology, 01069 Dresden, Germany.

Abstract. A large variety of long-lived radionuclides are present in ferromanganese crusts and can be used for the reconstruction of Earth's climate or the discovery of astrophysical events in Earth's past. Here, we present a selection of long-lived radionuclides that can be measured in ferromanganese crusts by accelerator mass spectrometry (AMS). The recent discoveries of cosmogenic as well as interstellar radionuclide anomalies within the last 10 million years showcase the scientific value of these geological archives. Technological developments, in particular in element separation chemistry to isolate radionuclides with e.g. a new rapid procedure for ¹⁰Be isolation as well as in measurement capabilities at the new Helmholtz Accelerator Mass Spectrometer Tracing Environmental Radionuclides (HAMSTER) will facilitate future investigations of a wide range of long-lived radionuclides.

1 Introduction

Ferromanganese crusts are slow-growing mineral deposits that form on the surfaces of seamounts or ridges in the world's oceans [1], where they grow by precipitation of iron and manganese oxides and hydroxides from seawater after colloid formation [2, 3]. Their exceptionally low growth-rates on the order of only a few millimetres per million years [4] make them unique long-term archives of past oceanic and climatic conditions, preserving a geochemical record of seawater composition and variations in trace and rare-earth element supply within their layered structures over several millions of years. A better understanding of their genesis as well as their location and sample-intrinsic variations is crucial for reconstructing the evolution of Earth's climate and ocean geochemistry on geological timescales. Beyond their scientific importance, ferromanganese crusts have gained increasing attention in recent years for their economic potential. They are enriched in critical metals such as cobalt, nickel, rare-earth elements, and platinum-group metals, all of which are in growing demand for new technologies and advanced industries [5]. Their slow growth, however, makes them a non-renewable resource and their mining poses unpredictable threats to the abyssal marine ecosystem. Recently, dark oxygen production through seawater electrolysis at the polymetallic surface of ferromanganese nodules was reported [6], making them a key component for aerobic abyssal organisms.

Radionuclides present in seawater are incorporated into ferromanganese crusts. Considering a crust's growth over millions of years, the half-life of interesting radionuclides should exceed ≈ 100 kyr. Prominent exceptions

are shorter-lived actinides such as ^{239,240}Pu or ^{245,246}Cm, in their case produced in and ejected by nuclear weapons testing and subsequently reaching Earth's oceans as local or global fallout. Abundances of these shorter-lived radionuclides in ferromanganese crusts serve as source identification through their isotopic ratios, while absolute concentrations are somewhat ambiguous due to the fact that most fallout is still within the water column and has not reached the seafloor yet [7]. Half-lives beyond 100 Myr are too long for radioactive decay to contribute significantly to changes in the radionuclide abundance over a crust's growth period. These radionuclides can be considered as quasi-stable isotopes for geochemical studies of the marine environment. Radionuclides with intermediate half-lives ($100 \text{ kyr} < t_{1/2} < 100 \text{ Myr}$) are ideal for dating the crusts as well as environmental monitoring and reconstruction of climatic as well as astrophysical events or trends. Dating of ferromanganese crusts is commonly achieved by isotopic systems [8], bio-stratigraphic [9] or magneto-stratigraphic [10] dating, or the decay of radionuclides with intermediate half-lives.

2 Radionuclides

In the following, a selection of different cosmogenic, interstellar and anthropogenic radionuclides and their abundances in ferromanganese crusts are discussed. The residence times of the discussed radionuclides in the ocean, which could lead to indistinct time profiles in ferromanganese crusts, are typically orders of magnitude shorter than their half-life and the timescale of a crust's growth. The measurement of these long-lived radionuclides is achieved by accelerator mass spectrometry (AMS) [11], an analytical single-atom counting technique with supe-

*e-mail: d.koll@hzdr.de dominik.koll@anu.edu.au



Figure 1. The ferromanganese crust VA13/2-237KD from the Central Pacific Ocean. This crust is arguably the best studied ferromanganese crust sample in the world. Reprinted with permission from Elsevier.

rior sensitivity due to the destruction of molecular interferences through the electron stripping process in the tandem accelerator. Here, the well-studied ferromanganese crust VA13/2-237KD (Figure 1) is taken as an example, representing a typical hydrogenetic ferromanganese crust from the Central Pacific Ocean (09°N, 146°W).

2.1 ^{10}Be

The cosmogenic radionuclide ^{10}Be ($t_{1/2} = 1.4$ Myr [13, 14]) is produced in the atmosphere by high-energy spallation reactions of primary and secondary cosmic rays on air molecules. Within 1–2 yr, ^{10}Be precipitates out of the atmosphere [15, 16] and reaches the ocean. After several hundred years [17, 18], beryllium reaches the seafloor and gets incorporated into sediments and ferromanganese encrustations.

The half-life of ^{10}Be as well as its steady production over long timescales and its reliable incorporation into ferromanganese crusts makes it the prime candidate for cosmogenic radionuclide dating over several million years. Dating of ferromanganese crusts with ^{10}Be was shown [12, 19] to be possible with high accuracy e.g. at the DREsden AMS (DREAMS) facility [20], see Figure 2 for two ^{10}Be concentration profiles of VA13/2-237KD over more than 10 half-lives of ^{10}Be . The highly efficient measurements as well as the high concentration of ^{10}Be in ferromanganese crusts lead to typical measurement times of about 30 minutes per sample. The time consuming bottleneck of ^{10}Be AMS is the chemical isolation of ^{10}Be which requires wet chemistry involving concentrated mineral acids.

In order to reduce processing times, the established chemical procedures for ferromanganese crusts [19, 21] were significantly shortened to: dissolution of 20 mg of pulverized crust in concentrated HCl with drops of H_2O_2 over 2 h, $500\ \mu\text{g}$ ^9Be carrier addition followed by hydroxide precipitation with ammonia and then drying and calcining at 900°C . This short procedure reduces the isobar ^{10}B and abundant manganese during the hydroxide precipitation, however, retains iron in the beryllium fraction. Considering iron abundances of 10%–20%

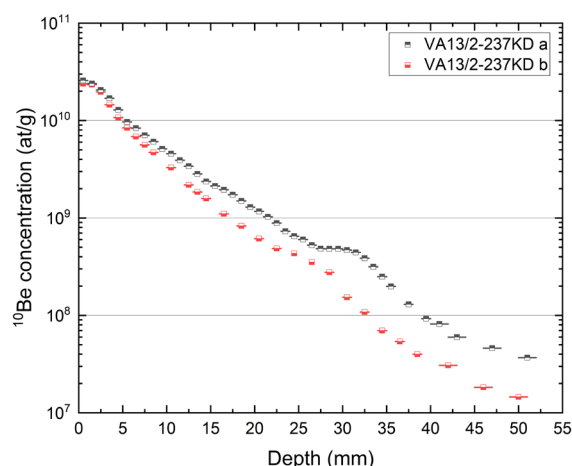


Figure 2. Two ^{10}Be concentration depth profiles in VA13/2-237KD. The ^{10}Be concentrations decline smoothly with depth and exhibit a ^{10}Be anomaly [12] at different depth, however, at the same time period. The crust was dated using these cosmogenic ^{10}Be profiles to more than 15 Myr. Reprinted from Koll et al. [12].

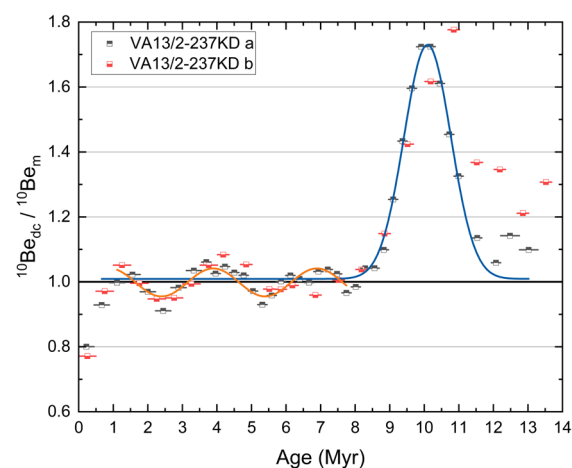


Figure 3. The late Miocene ^{10}Be anomaly [12]. The origin of the anomaly peaking at 10.1 Myr is currently unknown with terrestrial as well as astrophysical causes discussed. Reprinted from Koll et al. [12].

in ferromanganese crusts, 20 mg of crust powder yields 2–4 mg of Fe which dilutes the Be fraction, however, still yields sufficient beam intensity for AMS measurements. Measurements of fully processed samples as well as samples processed with this new short prescription agreed within 1% in their concentration. This reduced procedure requires less than 2 days in contrast to almost 2 weeks for the full procedure at the cost that only ^{10}Be can be analysed. Nevertheless, this shortened procedure enables a rapid scan of a large number of ferromanganese crust samples for their ^{10}Be concentration and therefore their age. The sampling of ferromanganese crusts for ^{10}Be (or other radionuclide) analysis typically requires the fixation of the crust in epoxy resin to establish a reference

frame and to stabilize the crust. Manual scraping or cutting is not recommended due to the irregular surface of ferromanganese crusts and a required reproducible depth resolution for accurate depth profiles. Sampling below 1 mm thickness is also not recommended due to pore water, diffusion and the granularity of the crust's surface that is usually covered by botryoids of larger dimensions. Note, studies of ^{230}Th ($t_{1/2} = 75.4$ kyr) in ferromanganese crusts [22–24] regularly sample ferromanganese crusts at the tens to hundreds of μm scale where special attention to such effects is necessary. Manually controlled or computer controlled milling in fixed geometry perpendicular to the crust's surface and with electronic depth measurements are recommended with a layer thickness of 1–2 mm per sample and a drill on the order of 10–20 mm in diameter [19].

Accurate and reproducible ^{10}Be measurements were the key to identify a cosmogenic ^{10}Be anomaly during the late Miocene [12], see Figure 3. The origin of this anomaly is unclear. A major ocean current reorganisation [25] as a possible terrestrial cause as well as astrophysical events such as supernovae [26] or the solar system's encounter with a cold cloud [27] were proposed as possible triggers for a ^{10}Be anomaly in ferromanganese crusts. Future measurements of other crust samples and deep-ocean sediments from various locations on Earth might shed light on the origin of the discovered anomaly. This ^{10}Be anomaly can already be used as a new independent time marker for the late Miocene in marine archives.

2.2 ^{26}Al

Cosmogenic ^{26}Al ($t_{1/2} = 0.7$ Myr [28]) is overall very similar to ^{10}Be . The low abundance of the target element argon in the atmosphere and the larger difference in nucleon number leads to a three orders of magnitude reduced production of ^{26}Al compared to ^{10}Be [29]. The shorter half-life of ^{26}Al on the one hand limits the dating of ferromanganese crusts to less than 10 Myr while on the other hand it could lead to a higher time resolution. In marine archives, a substantial in-situ component of ^{26}Al can be expected due to the $^{23}\text{Na}(\alpha, n)^{26}\text{Al}$ reaction on sodium from seawater with α -particles from uranium and thorium decay chains [30]. While attempts have been made [31] to employ ^{26}Al for dating of ferromanganese crusts, they are so far inconsistent with ^{10}Be dating, mostly because the in-situ component was not adequately considered. Future studies [32] could potentially establish ^{26}Al as a dating tool for ferromanganese crusts, however, it is hardly imaginable that it would surpass ^{10}Be dating. In-situ production will certainly limit the dating to shorter timescales (likely < 5 Myr) due to the increasing contribution of in-situ ^{26}Al with depth compared to decaying cosmogenic ^{26}Al .

Ferromanganese crusts would be promising archives to record an interstellar ^{26}Al influx [33]. The decay of galactic ^{26}Al with its characteristic γ -rays is, together

with ^{60}Fe , proof for ongoing nucleosynthesis in the galaxy [34]. To detect a minuscule surplus of interstellar ^{26}Al over the cosmogenic and in-situ baseline, highly accurate AMS measurements would be required with high statistics. This could become achievable by using AlO^- as molecular species in the AMS measurement which is one order of magnitude more intense than the regularly used anion. The use of the oxide anion, however, leads to isobaric interference from MgO^- which can be omitted by newly developed ion-laser interaction in a radiofrequency quadrupole [35]. The recently installed Helmholtz Accelerator Mass Spectrometer Tracing Environmental Radionuclides (HAMSTER) facility incorporates such a setup in the form of the Ion Linear Trap for Isobar Suppression (ILTIS).

Furthermore, the cross-section for the $^{23}\text{Na}(\alpha, n)^{26}\text{Al}$ reaction [36] should be remeasured to reliably model the in-situ production of ^{26}Al . An activation of sodium targets by a 0–10 MeV α -beam in combination with the offline AMS measurement of ^{26}Al is foreseen.

2.3 ^{53}Mn

Radionuclide dating of ferromanganese crusts beyond 15 Myr becomes challenging due to the advanced decay of ^{10}Be and ^{26}Al . The longer-lived cosmogenic radionuclide ^{53}Mn ($t_{1/2} = 3.7$ Myr [37]) would be ideal to date ferromanganese crusts over their whole growth period. The measurement of low levels of ^{53}Mn is notoriously difficult with neutron activation analysis to shorter-lived ^{54}Mn regularly being used in the past. It was shown that AMS at high terminal voltages and using a gas-filled magnet system [38–40] is capable of measuring ^{53}Mn at trace levels by sufficiently suppressing the stable isobar ^{53}Cr . The dating with ^{53}Mn , however, was never systematically established due to the lack of AMS facilities that meet the requirements for ^{53}Mn AMS.

Depth profiles of $^{53}\text{Mn}/\text{Mn}$ ratios were reported in four different ferromanganese crusts [40]. A piece of the ferromanganese crust VA13/2-237KD was dated by ^{10}Be [41] and this dating was then applied to an independently taken depth profile for ^{53}Mn analysis. Both age models obtained from ^{53}Mn and ^{10}Be were found to be in agreement considering the larger uncertainties from ^{53}Mn compared to precise ^{10}Be . The three other ferromanganese crusts were then dated with ^{53}Mn only. While no clear enhancement of ^{53}Mn above the predicted decay curve can be found in any time interval for the individual crusts, a statistical analysis of all four crusts found an enhancement around 2.6 Myr ago, the time period of previously reported interstellar ^{60}Fe deposition on Earth (see below). The statistical analysis used information from the ^{60}Fe profile in the crust VA13/2-237KD, i.e. the time period of the ^{60}Fe influx or the width of the peak. Considering the dating of the samples was based on the highly fluctuating ^{53}Mn data, possible temporal changes of the stable manganese abundance in the ocean and deep-ocean chemistry over millions of years leading to a varying $^{53}\text{Mn}/\text{Mn}$ base-level and that a

second ^{53}Mn influx related to the second ^{60}Fe influx (see below) was not found, an independent investigation of the claim of a discovered supernova-produced ^{53}Mn influx is urgently required. Higher sensitivity as well as precision might be achievable in the future using facilities such as HAMSTER with ILTIS to suppress the isobar ^{53}Cr .

2.4 ^{60}Fe

The supernova-produced interstellar radionuclide ^{60}Fe ($t_{1/2} = 2.6$ Myr [42, 43]) was several times successfully detected in ferromanganese crusts from the Pacific [44–47] as well as in deep-ocean sediments [45, 48], Antarctic snow [49] and lunar regolith [50]. Similar to ^{53}Mn , ^{60}Fe AMS still requires large accelerator facilities such as the recently decommissioned Munich accelerator lab [51] or the operational Heavy Ion Accelerator Facility (HIAF) at ANU, Australia [38]. The sensitivity, however, is several orders of magnitude higher due to the fact that the stable isobar ^{60}Ni can be effectively suppressed during chemistry and the favourable $\Delta Z = 2$ difference in proton number of the two isobars. Recent reviews cover the scientific merit of the detection of live interstellar radionuclides on Earth [11, 52].

The ferromanganese crust VA13/2-237KD was re-measured for ^{60}Fe covering more than 10 Myr of Earth's past [47]. Two distinct influx periods were discovered, in accordance with previous studies. The timings of both influx peaks, however, could be constrained to 2.4 Myr and 7.2 Myr due to the advanced sample characterization and ^{10}Be dating established in this project [19, 47].

2.5 ^{129}I

Studies of ^{129}I ($t_{1/2} = 16.1$ Myr [53]) in ferromanganese crusts are rare. While astrophysical models suggest that measurements of ^{129}I in ferromanganese crusts could strongly constrain heavy element nucleosynthesis in the universe [54], the terrestrial background as well as the intricate chemical behaviour of iodine in the ocean make it a challenging isotope to be analysed in deep-ocean archives. The release of ^{129}I by nuclear reprocessing plants dominates environmental levels and due to the porous structure of crusts, it could be transported into deeper layers overshadowing minuscule extraterrestrial amounts. Data in the literature [55, 56] suggests that not only ^{129}I poses challenges, but also stable iodine is highly variable from crust to crust but also within a depth profile of the same crust. It is likely that ^{129}I measurements in ferromanganese crusts are only meaningful for a carefully selected and characterized subset of samples.

2.6 ^{182}Hf

Another astrophysically interesting radionuclide is ^{182}Hf ($t_{1/2} = 8.9$ Myr [57]). In contrast to the other mentioned radionuclides, ^{182}Hf has an *s*-process as well as an *r*-process component making it a universal tracer for heavy element nucleosynthesis in the universe [58]. The measurement of interstellar ^{182}Hf with AMS is challenging

due to its abundant stable isobar ^{182}W and trace amounts of ^{182}Hf . The chemical extraction and isolation of hafnium from ferromanganese crusts is similarly challenging due to hafnium's chemical properties being a high-field-strength metal. Developments in chemical procedures [59] as well as in AMS measurements with ion-laser interaction [60] are ongoing to make a first measurement of interstellar ^{182}Hf possible.

2.7 Actinides

Natural as well as anthropogenic actinides are present in ferromanganese crusts. Plutonium isotopes were particularly studied for fallout isotopic ratios and recently for an interstellar ^{244}Pu signature [46, 47, 61]. The detection of anthropogenic as well as astrophysical plutonium by AMS is possible due to significant advancements in sample preparation, ion source as well as accelerator performance [19, 62] leading to detection efficiencies beyond 1:100 atoms. The defined time of release of plutonium to the terrestrial environment and the distribution of fallout plutonium in ferromanganese crusts can be used to investigate their porosity and the effect of pore water to radionuclide distributions within the crust. In VA13/2-237KD, the plutonium fallout signal extends down to about 10 mm depth, however, at greater depths than 3 mm the amount of plutonium is only at the percent level of the total inventory [47]. The search for a surplus in ^{244}Pu from astrophysical sources therefore requires the partitioning of the crust into a fallout layer and subsequent low level layers.

Other exemplary actinides measured in ferromanganese crusts are ^{230}Th , ^{231}Pa or $^{234,238}\text{U}$ [22–24, 63, 64]. In future studies, heavier actinides such as americium and curium will be analysed in ferromanganese crusts to complement the fallout inventory obtained from plutonium measurements.

3 Conclusion

Ferromanganese crusts are one of the most versatile environmental archives for radionuclides. Their growth over millions of years and their incorporation of virtually any radionuclide present in the environment makes them invaluable for scientific research. Accelerator mass spectrometry is an ideal approach to analyse ferromanganese crusts for several long-lived radionuclides.

References

- [1] J.R. Hein et al., Iron and manganese oxide mineralization in the Pacific, Geological Society, London, Special Publications **119**, 123 (1997), [10.1144/GSL.SP.1997.119.01.09](https://doi.org/10.1144/GSL.SP.1997.119.01.09)
- [2] P.E. Halbach, A. Jahn, G. Cherkashov, Marine Co-Rich Ferromanganese Crust Deposits: Description and Formation, Occurrences and Distribution, Estimated World-wide Resources, in *Deep-Sea Mining* (Springer International Publishing, 2017), pp. 65–141, ISBN 978-3-319-52557-0, [10.1007/978-3-319-52557-0_3](https://doi.org/10.1007/978-3-319-52557-0_3)

- [3] A. Koschinsky, P.E. Halbach, Sequential leaching of marine ferromanganese precipitates: Genetic implications, *Geochimica et Cosmochimica Acta* **59**, 5113 (1995). [10.1016/0016-7037\(95\)00358-4](https://doi.org/10.1016/0016-7037(95)00358-4)
- [4] J.R. Hein, A. Koschinsky, Deep-Ocean Ferromanganese Crusts and Nodules, in *Treatise on Geochemistry* (Elsevier, 2014), pp. 273–291, ISBN 978-0-08-098300-4, [10.1016/B978-0-08-095975-7.01111-6](https://doi.org/10.1016/B978-0-08-095975-7.01111-6)
- [5] P.A.J. Lusty, J.R. Hein, P. Josso, Formation and occurrence of ferromanganese crusts: Earth's storehouse for critical metals, *Elements* **14**, 313 (2018), [10.2138/gselements.14.5.313](https://doi.org/10.2138/gselements.14.5.313)
- [6] A.K. Sweetman, et al., Evidence of dark oxygen production at the abyssal seafloor, *Nature Geoscience* **17**, 737 (2024). [10.1038/s41561-024-01480-8](https://doi.org/10.1038/s41561-024-01480-8)
- [7] M. Nakano, P.P. Povinec, Modelling the distribution of plutonium in the Pacific Ocean, *Journal of Environmental Radioactivity* **69**, 85-106 (2003). [10.1016/S0265-931X\(03\)00088-2](https://doi.org/10.1016/S0265-931X(03)00088-2)
- [8] V. Klemm et al., Osmium isotope stratigraphy of a marine ferromanganese crust, *Earth and Planetary Science Letters* **238**, 42 (2005). [10.1016/j.epsl.2005.07.016](https://doi.org/10.1016/j.epsl.2005.07.016)
- [9] J.P. Cowen, E.H. DeCarlo, D.L. McGee, Calcareous nannofossil biostratigraphic dating of a ferromanganese crust from Schumann Seamount, *Marine Geology* **115**, 289 (1993). [10.1016/0025-3227\(93\)90057-3](https://doi.org/10.1016/0025-3227(93)90057-3)
- [10] H. Oda et al., Ultrafine-scale magnetostratigraphy of marine ferromanganese crust, *Geology* **39**, 227 (2011), [10.1130/G31610.1](https://doi.org/10.1130/G31610.1)
- [11] W. Kutschera et al., Atom counting with accelerator mass spectrometry, *Reviews of Modern Physics* **95**, 035006 (2023). [10.1103/RevModPhys.95.035006](https://doi.org/10.1103/RevModPhys.95.035006)
- [12] D. Koll et al., A cosmogenic ^{10}Be anomaly during the late Miocene as independent time marker for marine archives, *Nature Communications* **16**, 866 (2025). [10.1038/s41467-024-55662-4](https://doi.org/10.1038/s41467-024-55662-4)
- [13] G. Korschinek et al., A new value for the half-life of ^{10}Be by Heavy-Ion Elastic Recoil Detection and liquid scintillation counting, *Nuclear Instruments and Methods in Physics Research Section B: Beam Interactions with Materials and Atoms* **268**, 187 (2010). [10.1016/j.nimb.2009.09.020](https://doi.org/10.1016/j.nimb.2009.09.020)
- [14] J. Chmeleff et al., Determination of the ^{10}Be half-life by multicollector ICP-MS and liquid scintillation counting, *Nuclear Instruments and Methods in Physics Research Section B: Beam Interactions with Materials and Atoms* **268**, 192 (2010). [10.1016/j.nimb.2009.09.012](https://doi.org/10.1016/j.nimb.2009.09.012)
- [15] L.R. McHargue, P.E. Damon, The global ^{10}Be cycle, *Reviews of Geophysics* **29**, 141 (1991), [10.1029/91RG00072](https://doi.org/10.1029/91RG00072)
- [16] J.K. Willenbring, F. von Blanckenburg, Meteoric cosmogenic beryllium-10 adsorbed to river sediment and soil: Applications for Earth-surface dynamics, *Earth-Science Reviews* **98**, 105 (2010). [10.1016/j.earscirev.2009.10.008](https://doi.org/10.1016/j.earscirev.2009.10.008)
- [17] G.M. Raisbeck et al., ^{10}Be concentration and residence time in the deep ocean, *Earth and Planetary Science Letters* **51**, 275 (1980). [10.1016/0012-821X\(80\)90210-1](https://doi.org/10.1016/0012-821X(80)90210-1)
- [18] F. von Blanckenburg et al., Global distribution of beryllium isotopes in deep ocean water as derived from Fe-Mn crusts, *Earth and Planetary Science Letters* **141**, 213 (1996). [10.1016/0012-821X\(96\)00059-3](https://doi.org/10.1016/0012-821X(96)00059-3)
- [19] D. Koll et al., Element separation chemistry and cosmogenic ^{10}Be -dating of a ferromanganese crust, *Nuclear Instruments and Methods in Physics Research Section B: Beam Interactions with Materials and Atoms* **530**, 53 (2022). [10.1016/j.nimb.2022.08.017](https://doi.org/10.1016/j.nimb.2022.08.017)
- [20] J. Lachner et al., Optimization of ^{10}Be measurements at the 6 MV AMS facility DREAMS, *Nuclear Instruments and Methods in Physics Research Section B: Beam Interactions with Materials and Atoms* **535**, 29 (2023). [10.1016/j.nimb.2022.11.008](https://doi.org/10.1016/j.nimb.2022.11.008)
- [21] S. Fichter et al., Case studies of three geological archives for rare radionuclide measurements using accelerator mass spectrometry, *Frontiers in Environmental Chemistry* **5** (2024). [10.3389/fenvc.2024.1379862](https://doi.org/10.3389/fenvc.2024.1379862)
- [22] V. Banakar, D. Borole, Depth profiles of $^{230}\text{Th}_{\text{excess}}$, transition metals and mineralogy of ferromanganese crusts of the central indian basin and implications for palaeoceanographic influence on crust genesis, *Chemical Geology* **94**, 33 (1991). [10.1016/S0009-2541\(10\)80015-4](https://doi.org/10.1016/S0009-2541(10)80015-4)
- [23] F. Chabaux et al., ^{238}U - ^{234}U - ^{233}Th chronometry of FeMn crusts: Growth processes and recovery of thorium isotopic ratios of seawater, *Geochimica et Cosmochimica Acta* **59**, 633 (1995). [10.1016/0016-7037\(94\)00379-Z](https://doi.org/10.1016/0016-7037(94)00379-Z)
- [24] C. Claude et al., U-Th chronology and paleoceanographic record in a Fe-Mn crust from the NE Atlantic over the last 700 ka, *Geochimica et Cosmochimica Acta* **69**, 4845 (2005). [10.1016/j.gca.2005.05.016](https://doi.org/10.1016/j.gca.2005.05.016)
- [25] D. Evangelinos et al., Late Miocene onset of the modern Antarctic Circumpolar Current, *Nature Geoscience* **17**, 165 (2024). [10.1038/s41561-023-01356-3](https://doi.org/10.1038/s41561-023-01356-3)
- [26] E. Maconi et al., The late Miocene ^{10}Be anomaly and the possibility of a supernova, *Astronomy and Astrophysics* **701**, L14 (2025). [10.1051/0004-6361/202556253](https://doi.org/10.1051/0004-6361/202556253)
- [27] M. Opher, A. Loeb, J.E.G. Peek, A possible direct exposure of the Earth to the cold dense interstellar medium 2–3 Myr ago, *Nature Astronomy* **8**, 983–990 (2024). [10.1038/s41550-024-02279-8](https://doi.org/10.1038/s41550-024-02279-8)
- [28] M.S. Basunia, A.M. Hurst, Nuclear data sheets for A = 26, *Nuclear Data Sheets* **134**, 1 (2016). [10.1016/j.nds.2016.04.001](https://doi.org/10.1016/j.nds.2016.04.001)
- [29] M. Auer et al., Cosmogenic ^{26}Al in the atmosphere and the prospect of a $^{26}\text{Al}/^{10}\text{Be}$ chronometer to date old ice, *Earth and Planetary Science Letters* **287**, 453 (2009). [10.1016/j.epsl.2009.08.030](https://doi.org/10.1016/j.epsl.2009.08.030)

- [30] P. Sharma, R. Middleton, Radiogenic production of ^{10}Be and ^{26}Al in uranium and thorium ores: Implications for studying terrestrial samples containing low levels of ^{10}Be and ^{26}Al , *Geochimica et Cosmochimica Acta* **53**, 709 (1989). [10.1016/0016-7037\(89\)90013-6](https://doi.org/10.1016/0016-7037(89)90013-6)
- [31] K. Dong et al., The initial exploration for ^{26}Al chronology in deep-sea ferromanganese crust, *Radiation Detection Technology and Methods* **7**, 297 (2023). [10.1007/s41605-023-00386-0](https://doi.org/10.1007/s41605-023-00386-0)
- [32] J. Feige et al., ^{26}Al and ^{10}Be in deep-sea deposits – re-evaluating their applicability for depositional age dating, submitted (2026).
- [33] J. Feige et al., Limits on supernova-associated $^{60}\text{Fe}/^{26}\text{Al}$ nucleosynthesis ratios from accelerator mass spectrometry measurements of deep-sea sediments, *Physical Review Letters* **121** (2018). [10.1103/PhysRevLett.121.221103](https://doi.org/10.1103/PhysRevLett.121.221103)
- [34] R. Diehl et al., The radioactive nuclei ^{26}Al and ^{60}Fe in the cosmos and in the solar system, *Publications of the Astronomical Society of Australia* **38** (2021). [10.1017/pasa.2021.48](https://doi.org/10.1017/pasa.2021.48)
- [35] J. Lachner et al., Highly sensitive ^{26}Al measurements by ion-laser-interaction mass spectrometry, *International Journal of Mass Spectrometry* **465**, 116576 (2021). [10.1016/j.ijms.2021.116576](https://doi.org/10.1016/j.ijms.2021.116576)
- [36] E.B. Norman et al., $^{26g,m}\text{Al}$ production cross sections from the $^{23}\text{Na}(\alpha,n)^{26}\text{Al}$ reaction, *Nuclear Physics A* **390**, 561 (1982). [10.1016/0375-9474\(82\)90283-4](https://doi.org/10.1016/0375-9474(82)90283-4)
- [37] M. Honda, M. Imamura, Half-life of Mn^{53} , *Physical Review C* **4**, 1182 (1971). [10.1103/PhysRevC.4.1182](https://doi.org/10.1103/PhysRevC.4.1182)
- [38] A. Wallner et al., Accelerator mass spectrometry with ANU's 14 million volt accelerator, *Nuclear Instruments and Methods in Physics Research Section B: Beam Interactions with Materials and Atoms* **534**, 48 (2023). [10.1016/j.nimb.2022.10.021](https://doi.org/10.1016/j.nimb.2022.10.021)
- [39] K. Knie, T. Faestermann, G. Korschinek, AMS at the munich gas-filled analyzing magnet system GAMS, *Nuclear Instruments and Methods in Physics Research Section B: Beam Interactions with Materials and Atoms* **123**, 128 (1997). [10.1016/S0168-583X\(96\)00753-7](https://doi.org/10.1016/S0168-583X(96)00753-7)
- [40] G. Korschinek et al., Supernova-produced ^{53}Mn on Earth, *Physical Review Letters* **125**, 031101 (2020). [10.1103/PhysRevLett.125.031101](https://doi.org/10.1103/PhysRevLett.125.031101)
- [41] C. Fitoussi et al., Search for supernova-produced ^{60}Fe in a marine sediment, *Physical Review Letters* **101**, 121101 (2008), [10.1103/PhysRevLett.101.121101](https://doi.org/10.1103/PhysRevLett.101.121101)
- [42] G. Rugel et al., New measurement of the ^{60}Fe half-life, *Physical Review Letters* **103**, 072502 (2009). [10.1103/PhysRevLett.103.072502](https://doi.org/10.1103/PhysRevLett.103.072502)
- [43] A. Wallner et al., Settling the Half-Life of ^{60}Fe : Fundamental for a Versatile Astrophysical Chronometer, *Physical Review Letters* **114**, 041101 (2015). [10.1103/PhysRevLett.114.041101](https://doi.org/10.1103/PhysRevLett.114.041101)
- [44] K. Knie et al., ^{60}Fe anomaly in a deep-sea manganese crust and implications for a nearby supernova source, *Physical Review Letters* **93**, 171103 (2004). [10.1103/PhysRevLett.93.171103](https://doi.org/10.1103/PhysRevLett.93.171103)
- [45] A. Wallner et al., Recent near-Earth supernovae probed by global deposition of interstellar radioactive ^{60}Fe , *Nature* **532**, 69 (2016). [10.1038/nature17196](https://doi.org/10.1038/nature17196)
- [46] A. Wallner et al., ^{60}Fe and ^{244}Pu deposited on Earth constrain the r-process yields of recent nearby supernovae, *Science* **372**, 742 (2021), [10.1126/science.aax3972](https://doi.org/10.1126/science.aax3972)
- [47] D. Koll, Ph.D. thesis, The Australian National University and TUD Dresden University of Technology (2023), [10.25911/5NJJB-YC98](https://doi.org/10.25911/5NJJB-YC98)
- [48] P. Ludwig et al., Time-resolved 2-million-year-old supernova activity discovered in Earth's microfossil record, *Proceedings of the National Academy of Sciences* **113**, 9232 (2016), [10.1073/pnas.1601040113](https://doi.org/10.1073/pnas.1601040113)
- [49] D. Koll et al., Interstellar ^{60}Fe in Antarctica, *Physical Review Letters* **123**, 072701 (2019). [10.1103/PhysRevLett.123.072701](https://doi.org/10.1103/PhysRevLett.123.072701)
- [50] L. Fimiani et al., Interstellar ^{60}Fe on the surface of the Moon, *Physical Review Letters* **116**, 151104 (2016). [10.1103/PhysRevLett.116.151104](https://doi.org/10.1103/PhysRevLett.116.151104)
- [51] D. Koll et al., Recent developments for AMS at the Munich tandem accelerator, *Nuclear Instruments and Methods in Physics Research Section B: Beam Interactions with Materials and Atoms* **438**, 180 (2019). [10.1016/j.nimb.2018.05.002](https://doi.org/10.1016/j.nimb.2018.05.002)
- [52] B.D. Fields, A. Wallner, Deep-sea and lunar radioisotopes from nearby astrophysical explosions, *Annual Review of Nuclear and Particle Science* **73**, 365 (2023). [10.1146/annurev-nucl-011823-045541](https://doi.org/10.1146/annurev-nucl-011823-045541)
- [53] E. García-Toraño et al., The half-life of ^{129}I , *Applied Radiation and Isotopes* **140**, 157 (2018). [10.1016/j.apradiso.2018.06.007](https://doi.org/10.1016/j.apradiso.2018.06.007)
- [54] W. Wang et al., Gamma-ray emission of ^{60}Fe and ^{26}Al radioactivity in our galaxy, *The Astrophysical Journal* **889**, 169 (2020). [10.3847/1538-4357/ab6336](https://doi.org/10.3847/1538-4357/ab6336)
- [55] K. Dong et al., The measurement of ^{129}I in ferromanganese crusts and aerosol samples with AMS at CIAE, *Nuclear Instruments and Methods in Physics Research Section B: Beam Interactions with Materials and Atoms* **353**, 16 (2015). [10.1016/j.nimb.2015.04.019](https://doi.org/10.1016/j.nimb.2015.04.019)
- [56] L. Ji et al., Measurement of ^{129}I in ferromanganese crust with AMS, *Acta Oceanologica Sinica* **34**, 31 (2015). [10.1007/s13131-015-0718-4](https://doi.org/10.1007/s13131-015-0718-4)
- [57] C. Vockenhuber et al., New half-life measurement of ^{182}Hf : Improved chronometer for the early solar system, *Physical Review Letters* **93**, 172501 (2004). [10.1103/PhysRevLett.93.172501](https://doi.org/10.1103/PhysRevLett.93.172501)
- [58] M. Lugaro et al., Stellar origin of the ^{182}Hf cosmochronometer and the presolar history of solar system matter, *Science* **345**, 650 (2014), [10.1126/science.1253338](https://doi.org/10.1126/science.1253338)
- [59] D. Koll et al., Recent progress on interstellar radionuclides on Earth and the Moon, *The European Physical Journal A* **61**, 101 (2025). [10.1140/epja/s10050-](https://doi.org/10.1140/epja/s10050-)

025-01554-0

- [60] M. Martschini et al., The quest for AMS of ^{182}Hf - why poor gas gives pure beams, EPJ Web of Conferences **232**, 02003 (2020). [10.1051/epjconf/202023202003](https://doi.org/10.1051/epjconf/202023202003)
- [61] A. Wallner et al., Abundance of live ^{244}Pu in deep-sea reservoirs on Earth points to rarity of actinide nucleosynthesis, Nature Communications **6**, 5956 (2015). [10.1038/ncomms6956](https://doi.org/10.1038/ncomms6956)
- [62] M.A.C. Hotchkis et al., Efficient formation of negative ions for plutonium ams, Nuclear Instruments and Methods in Physics Research Section B: Beam Interactions with Materials and Atoms **568**, 165869 (2025). [10.1016/j.nimb.2025.165869](https://doi.org/10.1016/j.nimb.2025.165869)
- [63] G.M. Henderson, K.W. Burton, Using ($^{234}\text{U}/^{238}\text{U}$) to assess diffusion rates of isotope tracers in ferromanganese crusts, Earth and Planetary Science Letters **170**, 169 (1999). [10.1016/S0012-821X\(99\)00104-1](https://doi.org/10.1016/S0012-821X(99)00104-1)
- [64] J. Fietzke et al., Protactinium determination in manganese crust VA13/2 by thermal ionization mass spectrometry (TIMS), Nuclear Instruments and Methods in Physics Research Section B: Beam Interactions with Materials and Atoms **149**, 353 (1999). [10.1016/S0168-583X\(98\)00912-4](https://doi.org/10.1016/S0168-583X(98)00912-4)